Inorganic Chemistry

Article

pubs.acs.org/IC

Uranium(IV) Halide (F^-, Cl^-, Br^-, and I^-) Monoarene Complexes

Dominik P. Halter, Henry S. La Pierre, Frank W. Heinemann, and Karsten Meyer*

Department of Chemistry and Pharmacy, Inorganic Chemistry, Friedrich-Alexander University Erlangen-Nürnberg (FAU), Egerlandstrasse 1, 91058 Erlangen, Germany

Supporting Information

ABSTRACT: The syntheses of four nearly isostructural uranium(IV) monoarene complexes, supported by the arene anchored tris(aryloxide) chelate, $[(^{Ad,Me}ArO)_3mes]^{3-}$, are reported. Oxidation of the uranium(III) precursor $[((^{Ad,Me}ArO)_3mes)U]$, **1**, in the presence of tetrahydrofuran (THF) results in THF coordination and distortion of the equatorial coordination sphere to afford the uranium(IV) η^6-arene complexes, $[((^{Ad,Me}ArO)_3mes)U(X)(THF)]$, **2−X−THF**, (where X = F, Cl, Br, or I) as their THF adducts. The solvate-free trigonally ligated $[((^{Ad,Me}ArO)_3mes)U(F)]$, **2−F**, was prepared and isolated in the absence of coordinating solvents for comparison.

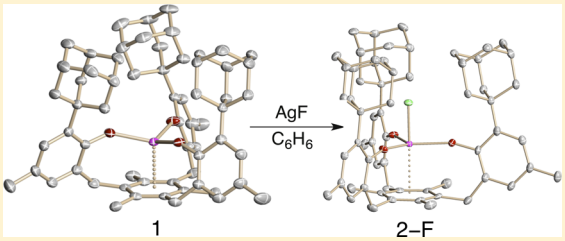

INTRODUCTION

Metal−arene complexes have played a key role in the development of bonding theory and now find a role as catalysts and reagents in organic synthesis for a variety of transformations.[1] Monoarene complexes of the lanthanides and actinides, however, remain quite rare.[2] While there has been extensive recent work on the electronic structure and reactivity of diuranium inverted arene complexes,[1a,3] a motif much more common for uranium than for the transition metals, relatively few monoarene complexes of uranium have been reported.[2a,4] In particular, and prior to our studies, examples of higher-oxidation state (i.e., uranium(IV)) monoarene complexes were limited to two related complexes $[U(C_6Me_6)Cl_2(\mu\text{-}Cl)_3UCl_2(C_6Me_6)]AlCl_4$ and $[U(C_6Me_6)Cl_2(\mu\text{-}Cl)_3UCl_2(\mu\text{-}Cl)_3UCl_2(C_6Me_6)]$.[4b,d] Due to the lability of the coordinated arene ligands in these complexes and their limited solubility in non-coordinating solvents, characterization was only achieved in the solid-state.

To fully evaluate the role of δ back-bonding in 5f metal arene complexes in the full spectrum of available uranium oxidation states, we have developed chelating tris(aryloxide) arene anchored ligands of the type $[(^{R,R'}ArO)_3mes]^{3-}$ (where R and R′ = *tert*-butyl or R = adamantyl and R′ = methyl).[4i,k] Due to the enforcement of the uranium−arene interaction through ligand constraints, the otherwise rather labile uranium−monoarene interaction is maintained in solution in these systems. Initial studies with the di-*tert*-butyl derivatized ligand revealed the role of δ back-bonding in these systems.[4i,j,5] However, in contrast to the parent $[((^{tBu,tBu}ArO)_3mes)U]$ complex, the first electrochemical evidence for a highly reactive formal, molecular uranium(II) complex was obtained with the development of the more sterically hindered adamantyl derivative $[((^{Ad,Me}ArO)_3mes)U]$, **1**.[4k,l] In order to further understand this remarkable redox behavior, the higher-valent uranium arene complexes were sought for comparison of arene bonding in uranium monoarene complexes and definition of the redox chemistry. To this end, the nearly isostructural uranium(IV) arene complexes bearing F^-, Cl^-, Br^-, and I^- ligands have been prepared (Scheme 1).

Scheme 1. Synthesis of Complexes 2−F (AgF, 3 d, 98%), 2−Cl (Excess DCM, 59%), 2−Br (Excess 1,2-DBE, 93%), and 2−I (0.5 equiv I_2, 92%), Starting from 1

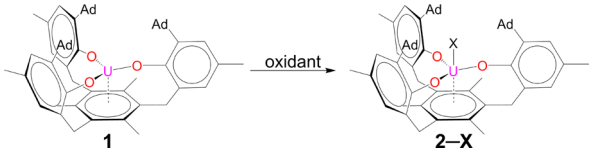

RESULTS AND DISCUSSION

Synthesis and X-ray Crystallography. Oxidation of **1** affords the uranium(IV) halide complexes $[((^{Ad,Me}ArO)_3mes)U(X)]$, **2−X** (where X = F^-, Cl^-, Br^-, or I^-), in good to excellent yields (Scheme 1). Exposure of **1** to AgF in THF gives **2−F** in 98% yield after pentane trituration (method A). The chloride complex, **2−Cl**, is prepared in 59% yield by the addition of a THF solution of **1** to an excess of dichloromethane (DCM). Similarly, the bromide complex, **2−Br**, is obtained by addition of **1** to excess 1,2-dibromoethane (DBE) in 93% yield. The iodide complex, **2−I**, is prepared in 92% yield via addition of 0.5 equiv of elemental iodine to **1**. All initially isolated complexes are obtained as powders as their desolvated, THF-free forms (as determined by ^1H NMR and EA). However, the use of THF was necessary to obtain single-crystals for XRD (X-ray diffraction) analysis. Consequently, complexes **2−X−THF** were obtained with coordinated THF in

Received: April 30, 2014
Published: August 1, 2014

   dx.doi.org/10.1021/ic501011p | *Inorg. Chem.* 2014, 53, 8418−8424

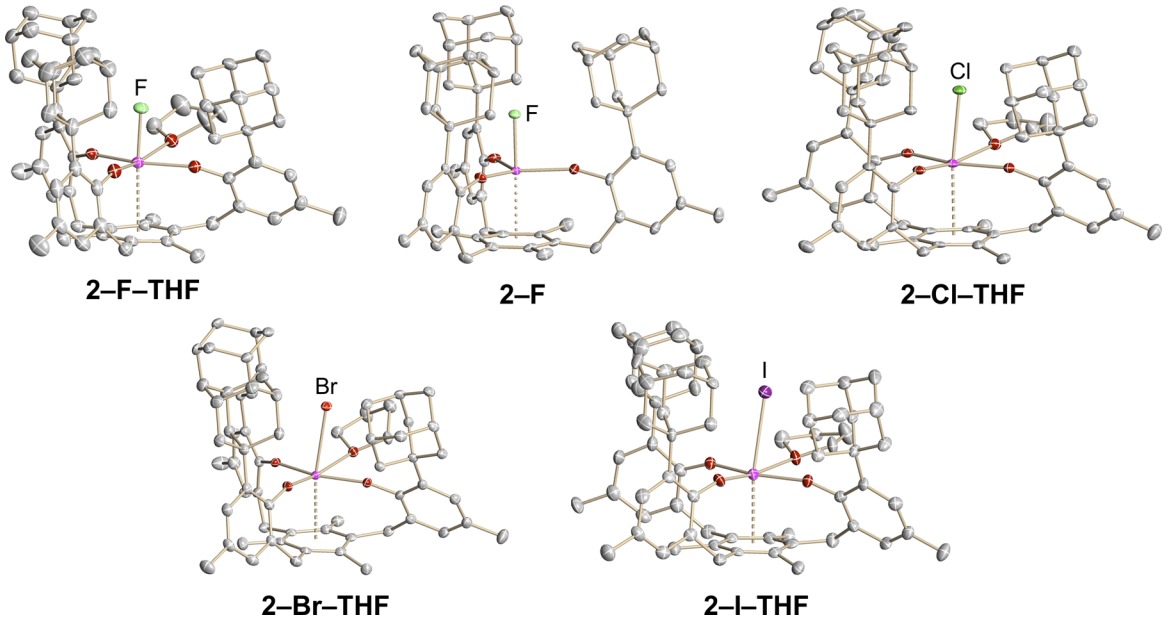

Figure 1. Molecular structures of **2–F–THF** (top, left) in crystals of $\{0.625[((^{Ad,Me}ArO)_3mes)U(F)(THF)]\cdot 0.375[((^{Ad,Me}ArO)_3mes)U(Cl)(THF)]\}\cdot 3C_5H_{12}$, obtained from a reaction of **2–Cl** with $Na[B(ArF_6)_4]$, (see Experimental Section), **2–F** (top, middle) in crystals of $[((^{Ad,Me}ArO)_3mes)U(F)]$, **2–Cl–THF** (top, right) in crystals of $[((^{Ad,Me}ArO)_3mes)U(Cl)(THF)]\cdot 1.5C_5H_{12}$, **2–Br–THF** (bottom, left) in crystals of $[((^{Ad,Me}ArO)_3mes)U(Br)(THF)]\cdot 3THF$, and **2–I–THF** (bottom, right) in crystals of $[((^{Ad,Me}ArO)_3mes)U(I)(THF)]\cdot C_5H_{12}$. Thermal ellipsoids are at 50% probability and co-crystallized solvents were omitted for clarity.

Table 1. Selected Bond Lengths (Å) and Angles (deg) for Complexes 2–F–THF, 2–F, 2–Cl–THF, 2–Br–THF, and 2–I–THF

structural params	2–F–THF	2–F	2–Cl–THF	2–Br–THF	2–I–THF
U–X	2.073(11)	2.076(2)	2.617(1)	2.8025(3)	3.0830(7)
U–arene$_{centr}$	2.666	2.559	2.657	2.645	2.664
U_{OOP}	−0.012(2)	−0.088(2)	−0.050(2)	−0.023(2)	−0.036(2)
U–O_{Ar} (av)	2.172	2.146	2.176	2.169	2.212
U–O_{THF}	2.601(4)		2.541(3)	2.591(3)	2.569(4)
U–C_{Ar} (av)	3.011	2.920	3.005	2.993	3.009
C_{Ar}–C_{Ar} (av)	1.404	1.407	1.405	1.406	1.416
X–U–arene$_{centr}$	175.4	179.2	172.1	170.8	168.5

their solid-state molecular structures (the structure of **2–F–THF** was obtained via an NMR reaction with **2–Cl–THF** and $Na[B(Ar^F{}_{24})_4]$ as a cocrystal with **2–Cl–THF**, *vide infra*). Only the fluoride complex, **2–F**, could be crystallized in the absence of THF, by the evaporation of a C_6D_6 solution of **2–F** into polyisobutenes. This solid-state molecular structure was obtained by an alternate synthetic method: specifically, the oxidation of **1** to **2–F** with AgF in benzene to obtain THF-free **2–F** in 93% yield. The solid-state molecular structures of these complexes were determined by single-crystal XRD studies (Figure 1, Table 1). Complexes **2–F–THF**, **2–Cl–THF**, **2–Br–THF**, and **2–I–THF** show very similar molecular structures with a distorted equatorial coordination sphere, including a bound THF to give four oxygen atom donors in the equatorial plane (three aryloxide oxygens and a fourth oxygen from a coordinated THF molecule). The apical positions are occupied by the centroid of the mesityl ring and the corresponding halide in axial position *trans* to the arene.

The halide complexes **2–F–THF**, **2–Cl–THF**, and **2–Br–THF** crystallize in the monoclinic space group *C*2/*c* and **2–I–THF** in $P2_1/c$. In line with our goals, the principal coordination geometry of the ligand is essentially invariant on oxidation and is not dependent on the identity of the halide. Two metrics vary across the series: the U–X bond length increases down the period from F through I (X = F, 2.073(11) Å; Cl, 2.617(1) Å; Br, 2.8025(3) Å; I, 3.0830(7) Å). Similarly, the X–U–arene$_{centr}$ angle decreases down the period from F through I (X = F, 175.4°; Cl, 172.1°; Br, 170.8°; I, 168.5°). These trends are in accord with increased covalent radii of the halides on descending the period.

The metrics of the arene ligand anchor for **2–F–THF**, **2–Cl–THF**, **2–Br–THF**, and **2–I–THF** are nearly identical. The U–arene$_{centr}$ distances span the narrow range from 2.65 to 2.67 Å, the U–C_{Ar}(ave) bond lengths vary from 2.99 to 3.01 Å, and the C_{Ar}–C_{Ar} (av) distances are observed between 1.40 and 1.42 Å. Since the free ligand has a C_{Ar}–C_{Ar} (av) bond length of 1.42 Å, no reduction of the arene is indicated from the analysis of the molecular structures in the solid-state.[4k] The uranium ion in **2–F–THF**, **2–Cl–THF**, **2–Br–THF**, and **2–I–THF** lies just below the plane defined by the oxygen atoms of the aryloxides (between −0.01 and −0.05 Å), while the coordinated THF is oriented above the plane (between +0.30 and +0.45 Å). The two previously reported uranium arene complexes prepared by Cotton and co-workers present similar metrics with U–C_{Ar} (av) of 2.92 Å, suggesting that the soluble

dx.doi.org/10.1021/ic501011p | *Inorg. Chem.* 2014, 53, 8418–8424

and stable complexes **2−X** possess similar bonding characteristics.[4b,d]

In contrast to complexes **2−X−THF**, solvent-free **2−F** possesses a trigonal coordination sphere in the solid-state with nearly equivalent U−C_{Ar} bonds at 2.92 Å, a U−$arene_{centr}$ distance of 2.56 Å, and C_{Ar}−C_{Ar} (av) bond length of 1.41 Å. Like the other uranium(IV) arene complexes in this series, the uranium ion lies only slightly below the plane defined by the aryloxide oxygen atoms (0.088(2) Å). The smaller size of the fluoride in **2−F** compared to the amide in the previously reported [((^{tBu,tBu}ArO)$_3$mes)U(dbabh)] (Hdbabh = 2,3:5,6-dibenzo-7-azabicyclo[2.2.1]hepta-2,5-diene)[6] indicates that the non-axial orientation of the amide in [((^{tBu,tBu}ArO)$_3$mes)U(dbabh)] is likely due to steric, rather than electronic effects.[4i]

^{1}H NMR Studies. As expected for the THF-free complexes in approximate C_{3v} symmetry (solvent-free materials were obtained by rigorous trituration, see the Experimental Section), all complexes present between 6 and 9 paramagnetically shifted and broadened resonances in their ^{1}H NMR spectra (recorded in C_6D_6), ranging from approximately 25 to −37 ppm (Figure 2). The ^{1}H NMR spectrum of **2−F** was assigned by ^{1}H, ^{13}C

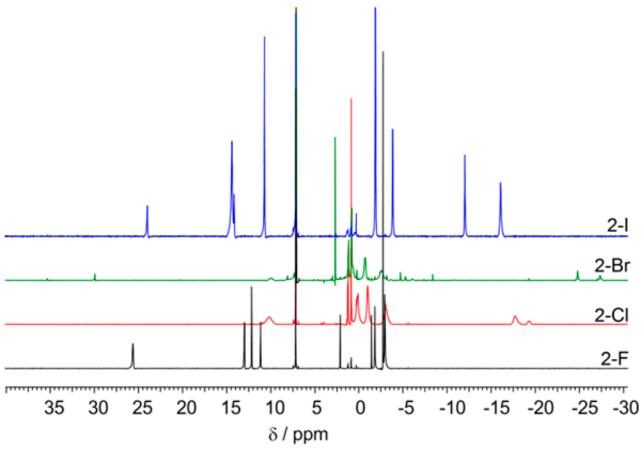

Figure 2. From bottom to top: ^{1}H NMR spectra of **2−F** (black), **2−Cl** (red), **2−Br** (green), and **2−I** (blue) in C_6D_6.

Dept135, 2D ^{1}H,^{1}H-COSY, and HMQC (see Supporting Information Figures S9−S26 for details). As previously reported for adamantyl aryloxide supported uranium complexes,[7] the variable number of observed resonances is due to overlap and accidental degeneracy of the adamantyl methylene protons. Accordingly, a VT NMR study of **2−F** was performed to assess whether the resonances coalesce at higher temperature (Figure 3). In the observable temperature range (25−90 °C), partial coalesence was indeed observed, suggesting a higher barrier for the adamantyl rotation in the fluoride complex in comparison to the heavier halides.[8] However, the overall rotation barrier results of two competing effects, namely the competing trends of increasing ionic radii and bond distance in the halide series.

A titration experiment of the solvate-free **2−F** (prepared by method B) with 0.1 to 200 equiv of THF in C_6D_6 was performed, but revealed no distinct change in the solution symmetry of the compound, according to the number of signals and their relative integration (i.e., there are still just two peaks corresponding to the methyl groups of the aryloxide arms and mesityl backbone in a 1:1 ratio) in the spectra (see Supporting Information Figure S6). From this titration experiment a

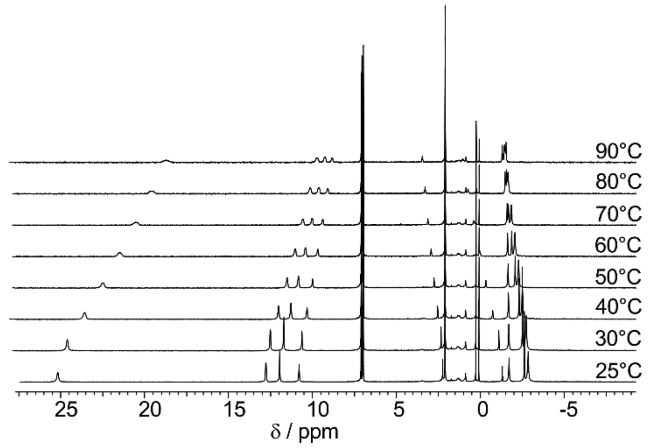

Figure 3. VT ^{1}H NMR spectra of **2−F** (after trituration) from 25 to 90 °C in toluene-d_8.

formation constant for the compound **2−F−THF** of K_{UTHF} = 9.67 was obtained for the fast exchange equilibrium with **2−F** (see Supporting Information for details).[9] As Figure 2 reveals, none of the compounds show signals corresponding to THF in their ^{1}H NMR spectra after trituration with pentane. In contrast, the exemplary spectrum of crude **2−F** (method A) prior to the pentane titruation features slightly paramagnetically shifted THF signals (Figure 4), and no reduction in symmetry

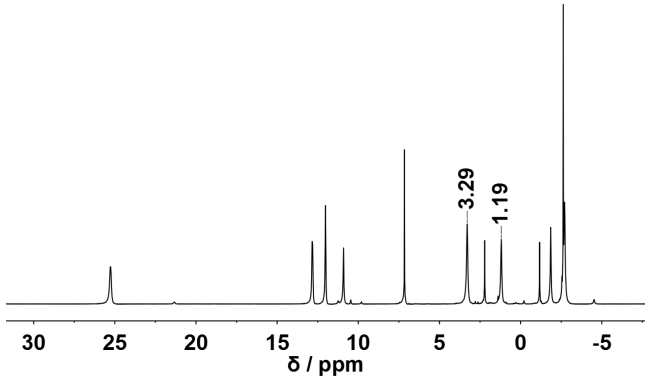

Figure 4. ^{1}H NMR spectrum of crude **2−F** (method A) in C_6D_6, before pentane trituration, see Experimental Section.

as expected from the THF titration results (Supporting Information). Thus, we conclude both that all complexes **2−X** were obtained THF-free after trituration, and that the presence of coordinating solvents like THF does not influence the solution geometry of these compounds on the NMR time scale.

The resonances attributable to **2−F** are shifted slightly in the presence of THF, as are the THF resonances, suggesting fast exchange on the NMR time scale.[8a,9] However, the apparent C_{3v} symmetry is retained through all concentrations of THF, implying that the distortion of the equatorial coordination sphere dominates in the solid-state only. These studies further indicate the absence of THF in the isolated complexes **2−F**, **2−Cl**, **2−Br**, and **2−I**, which were employed for all characterization methods other than XRD.[4g]

Chloride abstraction in **2−Cl** was attempted with Na[B(Ar^F_6)$_4$] (sodium tetrakis[(3,5-trifluoromethyl)phenyl]borate). Initial chloride abstraction and subsequent fluoride abstraction from the [B(Ar^F_6)$_4$]$^-$ anion yields **2−F** in nearly quantitative

dx.doi.org/10.1021/ic501011p | Inorg. Chem. 2014, 53, 8418−8424

conversion (as ascertained by NMR spectroscopy, see Figure 5). The reaction was followed by ^{1}H and ^{19}F NMR

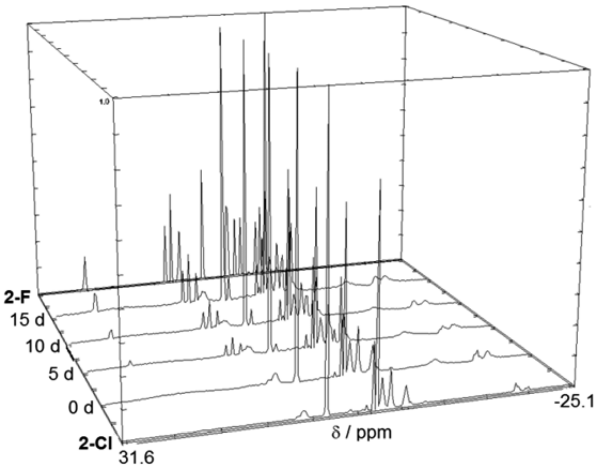

Figure 5. ^{1}H NMR stack-plot of the conversion of **2−Cl** to **2−F** in C_6D_6.

spectroscopy. The stack-plot in Figure 5 shows the appearance and growth of 3 signals around 12 ppm and a singlet at 25.41 ppm; both features are characteristic for the conversion of **2−Cl** with subsequent formation of **2−F**. ^{19}F NMR spectroscopy of the reaction mixture showed low intensity signals of the decomposition products of the $[B(ArF_6)_4]^-$ anion between −62 and −64 ppm and a high intensity $NaBArF_{24}$ signal at −63.51 ppm.[10] The ^{19}F NMR signal of the uranium fluoride was observed at −465.31 ppm in the reaction mixture, in agreement with that of the independently synthesized, pure fluoride complex **2−F**. This value is in good agreement with the results of Kanellakopulos et al., who observed the ^{19}F NMR signal for their Cp_3U-F at −420 ± 5 ppm.[11] It should be emphasized that these results indicate the applicability of the reported uranium(IV) complexes, for the cleavage of sp^3 C−F bonds.[12] The ability to generate a hydride complex would be necessary to render such a process catalytic.[13]

Electronic Absorption Spectroscopy. Effects of the axial ligand on the electronic structure were studied by vis−NIR experiments (0.01 M in THF). The compounds **2−Cl**, **2−Br**, and **2−I** feature 8 absorption bands for the f−f transitions (Figure 6 and Supporting Information Table S8) in the NIR region, with the band at ∼1050 nm showing two shoulders, which has previously been reported, but not assigned for U(IV) halide complexes in the literature.[11,14] Notably, the spectrum of the fluoride complex **2−F** presents with four more unique, sharp features with an increased molar extinction coefficient (up to 55 M^{-1} cm^{-1}). The complex **2−F** shows a strong bathochromic shift compared to the other halide compounds and also has a pronounced absorption band in the 2000 nm region.[15] Similar effects have been observed previously and, among other reasons, are likely due to a mixing of charge-transfer character into the f−f transitions.[16] Spectroscopic deviations from the other halides are very unlikely to be caused by different geometries in solution, as NMR studies indicate a consistent C_3-symmetric structure (*vide supra*).

Featuring a comparable band pattern, the electronic spectra of **2−Cl**, **2−Br**, and **2−I** demonstrate two clear trends: The first is the hypsochromic shift for the heavier homologues of the halides, indicating a reasonable contribution of ligand field

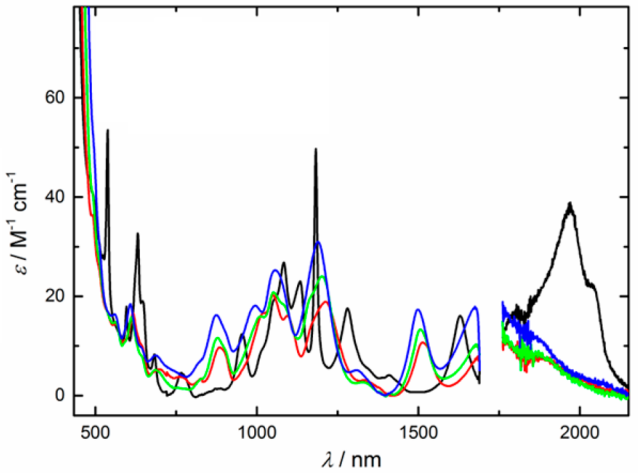

Figure 6. Comparative vis−NIR plot of the uranium halides **2−F** (black), **2−Cl** (red), **2−Br** (green), and **2−I** (blue), 0.01 M in THF.

splitting to the mostly spin−orbit coupling dominated electronic structure of uranium complexes.[17] This trend was also found for uranium(V) imido halides, $[Cp^*_2U(X)(NR)]$ (where R = 2,4,6-tBu_3-C_6H_2 or 2,6-$iPr_2C_6H_3$).[16a] It is noteworthy that although the relative intensities vary, the spectral region for the f−f transitions of **2−Cl**, **2−Br**, and **2−I** exhibits a pattern quite comparable to the uranium(IV) compounds Cp_3U-X (X = Cl, Br, I).[11] The second trend observed is the increase of the absorption intensities from **2−Cl** to **2−I**, due to a relaxation of the selection rules for complexes in a weaker crystal field.[16a]

SQUID Magnetometry. In temperature dependent SQUID measurements, complexes **2−Cl**, **2−Br**, and **2−I** behave almost identically (Figure 7). At 2 K, magnetic moments, μ_{eff}, of 0.38,

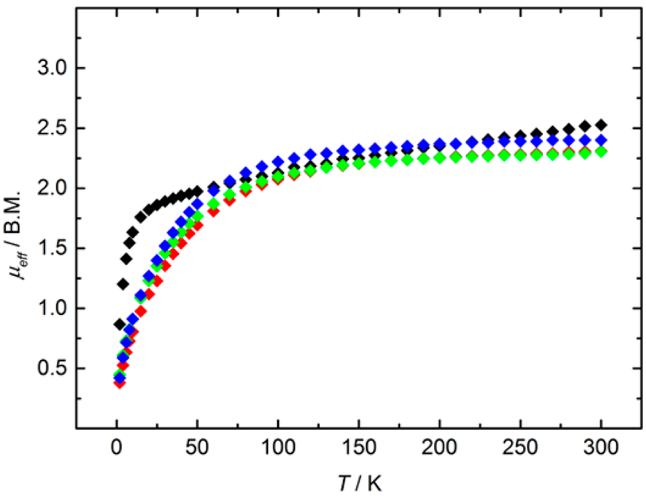

Figure 7. Temperature dependent SQUID measurements (at 5 T, but are field independent) from powdered samples of **2−F** (black), **2−Cl** (red), **2−Br** (green), and **2−I** (blue) between 2 and 300 K.

0.45, and 0.42 μ_B for **2−Cl**, **2−Br**, and **2−I** were observed, which increase with increasing temperature to μ_{eff} = 2.31 μ_B (**2−Cl** and **2−Br**) and 2.40 μ_B (**2−I**) at 300 K. This behavior is prototypical TIP (temperature independent paramagnetism) for U(IV) complexes. For the fluoride complex **2−F**, however, a significantly higher μ_{eff} at 2 K is observed (0.87 μ_B), which

dx.doi.org/10.1021/ic501011p | *Inorg. Chem.* 2014, 53, 8418−8424

increases rapidly to 1.82 μ_B at 20 K, and then undergoes a saturated, nearly linear rise to 2.53 μ_B at 300 K.

Similar behavior is typically observed for other literature reported uranium fluorides, which is rationalized in terms of the shortest U−X bond distance and the strongest point charge in the halide series that results in the strongest ligand field. Therefore, the low-level excited states are thermally accessible at low temperature (i.e., the initial rapid rise with increasing temperature), and the higher excited states are, in turn, isolated, which results in the slow rise in μ_{eff} above 20 K.[11,16b,18]

CONCLUSIONS

In summary, this article reports the synthesis, as well as solution and solid-state characterization of the isostructural series of the uranium(IV) halide complexes [((^{Ad,Me}ArO)$_3$mes)U(X)] with X = F, Cl, Br, and I. In the presence of THF, the C_3 symmetric complexes crystallize as [((^{Ad,Me}ArO)$_3$mes)U(X)(THF)], with a THF bound in the equatorial plane. Solution ^{1}H NMR studies indicate that the complexes lose coordinated THF under vacuum and are present as C_{3v} symmetric complexes in solution. This chelate-supported stability of the uranium−arene interaction is in contrast to the few known uranium(IV) monoarene complexes and allows the direct comparison of these canonical examples of uranium(IV) with the recently reported uranium(III) and formal uranium(II) species. In this respect, it is important to note that while the uranium arene interaction is maintained, the valence electronic structure, as indicated by electronic absorption spectra and SQUID magnetometry, is not significantly perturbed in comparison to the triazacyclononane supported uranium(IV) complexes. This parallel sets the stage for a qualitatively calibrated X-ray absorption study to examine the bonding of the arene across uranium oxidation states. Additionally, the abstraction of the axially bound supporting halide ligand results in the formation of a highly reactive species, capable of C−F bond activation.

EXPERIMENTAL SECTION

General Considerations. All air- and moisture-sensitive experiments were performed under dry nitrogen atmosphere using standard Schlenk techniques or in MBraun inert-gas gloveboxes containing an atmosphere of purified dinitrogen. The glovebox is equipped with a −35 °C freezer. Solvents were purified using a two-column solid-state purification system (Glass Contour System, Irvine, CA), transferred to the glovebox without exposure to air, and stored over molecular sieves and sodium (where appropriate). All glassware was dried by storage in an oven overnight (>8 h) at a temperature >160 °C. Celite was dried in an oven for a minimum of 3 d at a temperature >160 °C. NMR solvents were obtained packaged under argon and stored over activated molecular sieves and sodium (where appropriate) prior to use. [((^{Ad,Me}ArO)$_3$mes)U] was prepared according to literature procedures.[4k] All other reagents were acquired from commercial sources and used as received.

^{1}H NMR spectra were recorded on a JEOL ECX 400 or JEOL ECX 270 instrument at a probe temperature of 23 °C. Chemical shifts, δ, are reported relative to residual ^{1}H resonances of the solvent in ppm. ^{19}F NMR spectra were recorded on a JEOL ECX 400 instrument at a probe temperature of 23 °C with external reference. VT NMR experiments were carried out on a JEOL ECX 400 between 25 and 90 °C. To rule out temperature induced decomposition, a final spectrum was recorded at room temperature. Electronic absorption spectra were recorded from 250 to 2200 nm (Shimadzu, UV-3600) in the indicated solvent at room temperature. Infrared (IR) spectra were recorded on a Shimadzu Affinity-1 CE FTIR instrument from 400 to 4000 cm^{-1}. Solid samples of the compounds were homogenized with excess amount of KBr, and a pressed pellet was measured at room temperature. Elemental analyses were obtained using Euro EA 3000 (Euro Vector) and EA 1108 (Carlo-Erba) elemental analyzers in the Chair of Inorganic Chemistry at the University Erlangen-Nuremberg (Erlangen, Germany). Due to local ordinance, elemental analysis of fluorine containing uranium complexes is prohibited. SQUID magnetization data of powdered samples were recorded with a SQUID magnetometer (Quantum Design) at 5 kOe between 2 and 300 K for all samples. Values of the magnetic susceptibility were corrected for the underlying diamagnetic increment by using tabulated Pascal constants and the effect of the blank sample holders (gelatin capsule/straw).[19] Diamagnetic corrections (χ_{dia} [10^{-6} cm^3 mol^{-1}]) used for the complexes are **2−F** (−664.21), **2−Cl** (−678.01), **2−Br** (−688.51), and **2−I** (−702.51). Samples used for magnetization measurement were checked for chemical composition and purity by elemental analysis (C, H, and N) (except for **2−F**, clean ^{1}H NMR in the diamagnetic region and only 1 signal in ^{19}F NMR demonstrate spectroscopic purity in this case, see Supporting Information Figures S7 and S8) and ^{1}H NMR spectroscopy. Data reproducibility was also checked by obtaining data on two independently synthesized samples.

Synthesis of 2−F. [((^{Ad,Me}ArO)$_3$mes)UF] (Method A). To a solution of [((^{Ad,Me}ArO)$_3$mes)U] (57.0 mg, 0.0509 mmol) in THF (10 mL) was added AgF (6.4 mg, 0.0509 mmol) in one portion. The reaction mixture was stirred vigorously for 3 d and then filtered through Celite. The volatiles were removed *in vacuo* to yield a green powder. The residue was triturated with pentane (3 × 5 mL) to give the desolvated title compound in 98% yield (57.0 mg, 0.0501 mmol). ^{1}H NMR (400 MHz, C_6D_6, RT): −2.93 (br s, Ad-CH_2, 18 H), −2.73 (s, Ar-CH_3, 9 H), −1.84 (s, Ad-CH, 9 H), −1.46 (s, Ar-H, 3 H), 2.06 (s, Ar-CH, 3 H), 11.21 (s, Ar-CH_2-Ar, 6 H), 12.32 (s, Ar-CH_3, 9 H), 13.17 (d, J = 3 Hz, Ad-CH_2, 9 H), 25.92 (br s, Ad-CH_2, 9 H) ppm. ^{19}F NMR (400 MHz, C_6D_6, RT): −442.49 ppm, fwhm = 2.2 Hz. IR: 2900 (vs), 2846 (s), 1560 (w), 1446 (s), 1230 (vs), 1184 (w), 1161 (m), 1101 (w), 1086 (m), 1022 (w), 835 (m), 806 (s), 518 (s), 482 (m) U−F stretch,[20] 412 (w).

Synthesis of 2−F. [((^{Ad,Me}ArO)$_3$mes)UF] (Method B). To a solution of [((^{Ad,Me}ArO)$_3$mes)U] (28.5 mg, 0.0254 mmol) in benzene (10 mL) was added solid AgF (3.2 mg, 0.0252 mmol). The reaction mixture was stirred vigorously for 5 d and then filtered through Celite. The volatiles were removed *in vacuo* to yield the title compound as a green powder in 93% yield (27.0 mg, 0.0237 mmol). Slow evaporation (into X-ray oil) of a C_6D_6 solution of **2−F** at room temperature afforded crystals for XRD studies. ^{1}H NMR (270 MHz, C_6D_6, RT): −2.97 (br s, Ad-CH_2, 18 H), −2.82 (s, Ar-CH_3, 9 H), −1.89 (s, Ad-CH, 9 H), −1.47 (s, Ar-H, 3 H), 2.04 (s, Ar-CH, 3 H), 11.08 (s, Ar-CH_2-Ar, 6 H), 12.13 (s, Ar-CH_3, 9 H), 12.96 (d, J = 10.79 Hz, Ad-CH_2, 9 H), 25.62 (br s, Ad-CH_2, 9 H) ppm. IR: 2900 (vs), 2846 (s), 1446 (s), 1230 (vs), 1184 (w), 1161 (m), 1101 (w), 1086 (m), 1022 (w), 835 (s), 806 (s), 522 (s), 480 (m) U−F stretch,[20] 408 (w).

Synthesis of 2−Cl. [((^{Ad,Me}ArO)$_3$mes)UCl]. A solution of [((^{Ad,Me}ArO)$_3$mes)U] (60.0 mg, 0.0537 mmol) in THF (5 mL) was added dropwise to a vial charged with DCM (5 mL, excess) while stirring. The solvent was removed *in vacuo*, and the residue was washed with pentane to precipitate a yellow powder. The powder was filtered off and washed through the filter pipet with benzene. The volatiles were removed *in vacuo*. The residue was crystallized overnight from a saturated pentane solution with 2 drops of THF per 5 mL pentane stored at −35 °C. Decantation of the crystals, followed by removal the remaining volatiles, gave the desolvated title complex in 59% yield (36.6 mg, 0.0299 mmol). Recrystallization by the same method gave crystals appropriate for XRD studies of **2−Cl−THF**. ^{1}H NMR (270 MHz, C_6D_6, RT): −19.29 (br s, 2 H), −17.71 (br s, 8 H), −3.03 (br s, 15 H), −0.99 (br s, 20 H), −0.18 (br s, 20 H), 10.17 (br s, 10 H) ppm. Anal. Calcd for $C_{63}H_{75}ClO_3U$: C, 65.58, H, 6.55. Found: C, 65.32; H, 6.91. IR: 2900 (vs), 2846 (s), 1442 (s), 1222 (s), 1205 (s), 1182 (m), 1157 (s), 1018 (w), 852 (w), 819 (m), 802 (s), 518 (s), 416 (m).

Reaction of 2−Cl with Na[B(Ar$^F_6$)$_4$]. Na[B(Ar$^F_6$)$_4$] (11.5 mg, 0.0129 mmol) was added to a solution of [((^{Ad,Me}ArO)$_3$mes)UCl] (15.0 mg, 0.0130 mmol) in C_6D_6 (approximately 0.7 mL) inside a Teflon capped NMR tube. ^{1}H NMR spectra were recorded every 5

dx.doi.org/10.1021/ic501011p | Inorg. Chem. 2014, 53, 8418−8424

days to monitor the formation of **2−F** (see Figure 5). To grow single-crystals from the reaction mixture, the solvent was removed *in vacuo*, and a concentrated pentane solution of the reaction mixture with 2 drops of THF per 5 mL pentane was stored at −35 °C (the molecular structure obtained for **2−F−THF** with cocrystallized **2−Cl−THF** is presented in Figure 1 due to a higher quality of the data set compared to the one obtained from pure **2−F−THF**).

Synthesis of 2−Br. [((Ad,MeArO)$_3$mes)UBr]. A solution [((Ad,MeArO)$_3$mes)U] (23.0 mg, 0.0206 mmol) in THF (5 mL) was added dropwise to a vial charged with 1,2-dibromoethane (5 mL, excess) while stirring. The volatiles were removed *in vacuo* to yield a green solid. The crude product was triturated with pentane (2 × 5 mL), and the desolvated title compound was obtained as a green-yellow powder in 93% yield (23.0 mg, 0.0192 mmol). Storing a saturated pentane solution with 2 drops of THF per 5 mL pentane overnight at −35 °C afforded XRD quality crystals of **2−Br−THF**. ^{1}H NMR (270 MHz, C_6D_6, RT): −27.30 (br s, 7 H), −24.73 (br s, 8 H), −10.72 (br s, 19 H), −2.36 (br s, 16 H), −0.63 (br s, 12 H), 10.06 (br s, 13 H) ppm. Anal. Calcd for $C_{63}H_{75}BrO_3U$: C, 63.15, H, 6.31. Found: C, 62.61; H, 6.63 (consistently low carbon on multiple runs). IR: 2900 (vs), 2846 (s), 1444 (s), 1222 (s), 1203 (s), 1180 (m), 1155 (s), 1068 (w), 1018 (w), 854 (w), 800 (s), 516 (s).

Synthesis of 2−I. [((Ad,MeArO)$_3$mes)UI]. A solution of I_2 (4.3 mg, 0.0335 mmol) in benzene (2 mL) was added dropwise to a solution of [((Ad,MeArO)$_3$mes)U] (37.5 mg, 0.0335 mmol) in benzene (10 mL). The volatiles were removed *in vacuo* to yield a dingy, yellow solid. The residue was extracted with pentane (2 × 5 mL), and after removal of the volatiles *in vacuo*, the residue was recrystallized from a concentrated pentane solution with 2 drops of THF per 5 mL pentane at −35 °C. Decantation of the crystals, followed by removal the remaining volatiles, gave the desolvated title complex in 92% yield (38.4 mg, 0.0308 mmol). Recrystallization by the same method gave crystals appropriate for XRD studies of **2−I−THF**. Crystals obtained by this method were employed for HN analysis. ^{1}H NMR (270 MHz, C_6D_6, RT): −16.05 (br s, 8 H), −12.00 (br s, 6 H), −3.82 (br s, 10 H), −1.88 (br s, 19 H), 10.71 (br s, 9 H), 14.41 (br s, 20 H), 23.99 (br s, 3 H) ppm. Anal. Calcd for $C_{63}H_{75}IO_3U$·THF: C, 61.09, H, 6.35. Found: C, 61.33; H, 6.27. IR: 2900 (vs), 2846 (s), 1444 (s), 1220 (s), 1201 (s), 1180 (s), 1155 (s), 1101 (w), 1070 (w) 1016 (w), 852 (w), 817 (m), 798 (s), 516 (s), 410 (m).

Crystallographic Details. Suitable single-crystals of the investigated compounds were embedded in protective perfluoropolyalkylether oil and transferred to the cold nitrogen gas stream of the diffractometer. Intensity data for **2−F−THF**, **2−F**, **2−Cl−THF**, and **2−I−THF** were collected using Mo Kα radiation (λ = 0.710 73 Å) on a Bruker Kappa APEX 2 IμS Duo diffractometer equipped with QUAZAR focusing Montel optics. Intensity data for **2−Br−THF** were collected on a Bruker Smart APEX 2 diffractometer using Mo Kα radiation (λ = 0.710 73 Å, graphite monochromator). Data were corrected for Lorentz and polarization effects, and semiempirical absorption corrections were performed on the basis of multiple scans using *SADABS*.[21] The structures were solved by direct methods and refined by full-matrix least-squares procedures on F^2 using *SHELXTL NT* 6.12.[22] Refinement of **2−F** was carried out using *SHELXL-2013*.[23]

All non-hydrogen atoms were refined with anisotropic displacement parameters. All hydrogen atoms were placed in positions of optimized geometry, and their isotropic displacement parameters were tied to those of the corresponding carrier atoms by a factor of either 1.2 or 1.5. Crystallographic data, data collection, and structure refinement details are given in Supporting Information Tables S1 and S2. Molecular structures of the complexes (excluding hydrogen atoms, disorder, and solvent molecules) are depicted in Supporting Information Figures S1−S5. Bond distances and angles are listed in Supporting Information Tables S3−S7.

■ ASSOCIATED CONTENT

Supporting Information

Further crystallographic techniques and tables and further NMR details (CIF and PDF). This material is available free of charge via the Internet at http://pubs.acs.org. CCDC-991346 (for **2−F−THF**), CCDC-991347 (for **2−F**), CCDC-991348 (for **2−Cl−THF**), CCDC-991349 (for **2−Br−THF**), and CCDC-991350 (for **2−I−THF**) contain the supplementary crystallographic data for this Article. This data can be obtained free of charge via http://www.ccdc.cam.ac.uk/products/csd/request/ [or from Cambridge Crystallographic Data Centre, 12 Union Road, Cambridge, CB2 1EZ U.K. (fax, ++44-1223-336-033; e-mail, deposit@ccdc.cam.ac.uk)].

■ AUTHOR INFORMATION

Corresponding Author

*E-mail: karsten.meyer@fau.de.

Notes

The authors declare no competing financial interest.

■ ACKNOWLEDGMENTS

We would like to thank Dr. Andreas Schuerer for his help in acquiring VT-NMR spectra for **2−F**. The Bundesministerium für Bildung und Forschung (BMBF 2020+, 02NUK012C and 02NUK020C), the FAU Erlangen-Nürnberg, and COST Action CM1006 are acknowledged for financial support.

■ REFERENCES

(1) (a) Arnold, P. L.; Mansell, S. M.; Maron, L.; McKay, D. *Nat. Chem.* **2012**, *4*, 668−674. (b) Hubig, S. M.; Lindeman, S. V.; Kochi, J. K. *Coord. Chem. Rev.* **2000**, *200−202*, 831−873. (c) King, W. A.; Marks, T. J.; Anderson, D. M.; Duncalf, D. J.; Cloke, F. G. N. *J. Am. Chem. Soc.* **1992**, *114*, 9221−9223. (d) Kündig, E. P.; Xu, L.-H.; Kondratenko, M.; Cunningham, A. F.; Kunz, M. *Eur. J. Inorg. Chem.* **2007**, *2007*, 2934−2943. (e) Trifonova, E. A.; Perekalin, D. S.; Lyssenko, K. A.; Kudinov, A. R. *J. Organomet. Chem.* **2013**, *727*, 60−63. (f) Astruc, D. *Modern Arene Chemistry*; Wiley: Weinheim, 2002. (g) Astruc, D. *Tetrahedron* **1983**, *39*, 4027−4095.

(2) (a) Cotton, F. A.; Schwotzer, W. *Organometallics* **1987**, *6*, 1275−1280. (b) Cruz, C. A.; Emslie, D. J. H.; Robertson, C. M.; Harrington, L. E.; Jenkins, H. A.; Britten, J. F. *Organometallics* **2009**, *28*, 1891−1899. (c) Korobkov, I.; Gambarotta, S.; Yap, G. P. A. *Angew. Chem., Int. Ed.* **2003**, *42*, 814−818.

(3) (a) La Pierre, H. S.; Meyer, K. *Prog. Inorg. Chem.* **2014**, *58*, 303−416. (b) Diaconescu, P. L.; Arnold, P. L.; Baker, T. A.; Mindiola, D. J.; Cummins, C. C. *J. Am. Chem. Soc.* **2000**, *122*, 6108−6109. (c) Vlaisavljevich, B.; Diaconescu, P. L.; Lukens, W. L.; Gagliardi, L.; Cummins, C. C. *Organometallics* **2013**, *32*, 1341−1352. (d) Diaconescu, P. L.; Cummins, C. C. *J. Am. Chem. Soc.* **2002**, *124*, 7660−7661. (e) Diaconescu, P. L.; Cummins, C. C. *Inorg. Chem.* **2012**, *51*, 2902−2916. (f) Evans, W. J.; Kozimor, S. A.; Ziller, J. W.; Kaltsoyannis, N. *J. Am. Chem. Soc.* **2004**, *126*, 14533−14547. (g) Evans, W. J.; Traina, C. A.; Ziller, J. W. *J. Am. Chem. Soc.* **2009**, *131*, 17473−17481. (h) Monreal, M. J.; Khan, S. I.; Kiplinger, J. L.; Diaconescu, P. L. *Chem. Commun.* **2011**, *47*, 9119−9121. (i) Mills, D. P.; Moro, F.; McMaster, J.; van Slageren, J.; Lewis, W.; Blake, A. J.; Liddle, S. T. *Nat. Chem.* **2011**, *3*, 454−460. (j) Mougel, V.; Camp, C.; Pecaut, J.; Coperet, C.; Maron, L.; Kefalidis, C. E.; Mazzanti, M. *Angew. Chem., Int. Ed.* **2012**, *51*, 12280−12284. (k) Patel, D.; Moro, F.; McMaster, J.; Lewis, W.; Blake, A. J.; Liddle, S. T. *Angew. Chem., Int. Ed.* **2011**, *50*, 10388−10392. (l) Patel, D.; Tuna, F.; McInnes, E. J. L.; McMaster, J.; Lewis, W.; Blake, A. J.; Liddle, S. T. *Dalton Trans.* **2013**, *42*, 5224.

(4) (a) Cesari, M.; Pedretti, U.; Zazzetta, Z.; Lugli, G.; Marconi, W. *Inorg. Chim. Acta* **1971**, *5*, 439−444. (b) Cotton, A. F.; Schwotzer, W. *Organometallics* **1985**, *4*, 943−944. (c) Cotton, F. A.; Schwotzer, W.; Simpson, C. Q. *Angew. Chem., Int. Ed. Engl.* **1986**, *25*, 637−639. (d) Campbell, G. C.; Cotton, F. A.; Haw, J. F.; Schwotzer, W. *Organometallics* **1986**, *5*, 274−279. (e) Garbar, A. V.; Leonov, M. R.; Zakharov, L. N.; Struchkov, Y. T. *Russ. Chem. Bull.* **1996**, *45*, 451.

(f) Baudry, D.; Bulot, E.; Ephritikhine, M. *J. Chem. Soc., Chem. Commun.* **1988**, 1369−1370. (g) van der Sluys, W. G.; Burns, C. J.; Huffman, J. C.; Sattelberger, A. P. *J. Am. Chem. Soc.* **1988**, *110*, 5924−5925. (h) Evans, W. J.; Kozimor, S. A.; Hillman, W. R.; Ziller, J. W. *Organometallics* **2005**, *24*, 4676−4683. (i) Bart, S. C.; Heinemann, F. W.; Anthon, C.; Hauser, C.; Meyer, K. *Inorg. Chem.* **2009**, *48*, 9419−9426. (j) Lam, O. P.; Bart, S. C.; Kameo, H.; Heinemann, F. W.; Meyer, K. *Chem. Commun.* **2010**, *46*, 3137. (k) La Pierre, H. S.; Kameo, H.; Halter, D. P.; Heinemann, F. W.; Meyer, K. *Angew. Chem., Int. Ed.* **2014**, *53*, 7154−7157. (l) La Pierre, H. S.; Scheurer, A. S.; Hieringer, W.; Heinemann, F. W.; Meyer, K. *Angew. Chem., Int. Ed.* **2014**, *53*, 7158−7162.

(5) Castro, L.; Lam, O. P.; Bart, S. C.; Meyer, K.; Maron, L. *Organometallics* **2010**, *29*, 5504−5510.

(6) Carpino, L. A.; Padykula, R. E.; Barr, D. E.; Hall, F. H.; Krause, J. G.; Dufresne, R. F.; Thoman, C. J. *J. Org. Chem.* **1988**, *53*, 2565−2572.

(7) Nakai, H.; Hu, X. L.; Zakharov, L. N.; Rheingold, A. L.; Meyer, K. *Inorg. Chem.* **2004**, *43*, 855−857.

(8) (a) Bain, A. D. *Prog. Nucl. Magn. Reson. Spectrosc.* **2003**, *43*, 63−103. (b) Guo, W.; Brown, T. A.; Fung, B. M. *J. Phys. Chem.* **1991**, *95*, 1829−1836.

(9) Mehdoui, T.; Berthet, J. C.; Thuery, P.; Ephritikhine, M. *Dalton Trans.* **2004**, 579−590.

(10) (a) Yakelis, N. A.; Bergman, R. G. *Organometallics* **2005**, *24*, 3579−3581. (b) Weber, S. G.; Zahner, D.; Rominger, F.; Straub, B. F. *Chem. Commun.* **2012**, *48*, 11325.

(11) Fischer, R. D.; Ammon, R. V.; Kanellakopulos, B. *J. Organomet. Chem.* **1970**, *25*, 123−137.

(12) (a) Hu, M.; He, Z.; Gao, B.; Li, L.; Ni, C.; Hu, J. *J. Am. Chem. Soc.* **2013**, *135*, 17302−17305. (b) Klahn, M.; Rosenthal, U. *Organometallics* **2012**, *31*, 1235−1244. (c) Weydert, M.; Andersen, R. A.; Bergman, R. G. *J. Am. Chem. Soc.* **1993**, *115*, 8837−8838.

(13) (a) Johnson, S. A.; Huff, C. W.; Mustafa, F.; Saliba, M. *J. Am. Chem. Soc.* **2008**, *130*, 17278−17280. (b) Panisch, R.; Bolte, M.; Müller, T. *J. Am. Chem. Soc.* **2006**, *128*, 9676−9682. (c) Young, R. J.; Grushin, V. V. *Organometallics* **1999**, *18*, 294−296.

(14) Cantat, T.; Scott, B. L.; Morris, D. E.; Kiplinger, J. L. *Inorg. Chem.* **2009**, *48*, 2114−2127.

(15) Kosog, B.; La Pierre, H. S.; Denecke, M. A.; Heinemann, F. W.; Meyer, K. *Inorg. Chem.* **2012**, *51*, 7940−7944.

(16) (a) Graves, C. R.; Yang, P.; Kozimor, S. A.; Vaughn, A. E.; Clark, D. L.; Conradson, S. D.; Schelter, E. J.; Scott, B. L.; Thompson, J. D.; Hay, P. J.; Morris, D. E.; Kiplinger, J. L. *J. Am. Chem. Soc.* **2008**, *130*, 5272−5285. (b) Schelter, E. J.; Yang, P.; Scott, B. L.; Thompson, J. D.; Martin, R. L.; Hay, P. J.; Morris, D. E.; Kiplinger, J. L. *Inorg. Chem.* **2007**, *46*, 7477−7488. (c) Morris, D. E.; Da Re, R. E.; Jantunen, K. C.; Castro-Rodriguez, I.; Kiplinger, J. L. *Organometallics* **2004**, *23*, 5142−5153.

(17) (a) Bagus, P. S.; Ilton, E. S. *Top. Catal.* **2013**, *56*, 1121−1128. (b) Bagus, P. S.; Ilton, E. S.; Martin, R. L.; Jensen, H. J. A.; Knecht, S. *Chem. Phys. Lett.* **2012**, *546*, 58−62. (c) Rinehart, J. D.; Harris, T. D.; Kozimor, S. A.; Bartlett, B. M.; Long, J. R. *Inorg. Chem.* **2009**, *48*, 3382−3395.

(18) (a) Almond, P. M.; Deakin, L.; Mar, A.; Albrecht-Schmitt, T. E. *J. Solid State Chem.* **2001**, *158*, 87−93. (b) Almond, P. M.; Deakin, L.; Porter, M. J.; Mar, A.; Albrecht-Schmitt, T. E. *Chem. Mater.* **2000**, *12*, 3208−3213. (c) Gajek, Z.; Mulak, J.; Krupa, J. C. *J. Solid State Chem.* **1993**, *107*, 413−1427.

(19) Bain, G. A.; Berry, J. F. *J. Chem. Educ.* **2008**, *85*, 532−536.

(20) Bagnall, K. W.; Du Preez, J. G. H.; Gellatly, B. J.; Holloway, J. H. *J. Chem. Soc., Dalton Trans.* **1975**, 1963−1968.

(21) *SADABS*; Bruker AXS, Inc.: Madison, WI, 2002.

(22) *SHELXTL NT 6.12*; Bruker AXS, Inc.: Madison, WI, 2002.

(23) *SHELXL-2013*; Bruker AXS, Inc.: Madison, WI, 2013.